

Study of the decay $D_s^+ \rightarrow K^+ K^- e^+ \nu_e$

B. Aubert,¹ M. Bona,¹ Y. Karyotakis,¹ J. P. Lees,¹ V. Poireau,¹ E. Prencipe,¹ X. Prudent,¹ V. Tisserand,¹
J. Garra Tico,² E. Grauges,² L. Lopez^{ab,3}, A. Palano^{ab,3}, M. Pappagallo^{ab,3}, G. Eigen,⁴ B. Stugu,⁴ L. Sun,⁴
G. S. Abrams,⁵ M. Battaglia,⁵ D. N. Brown,⁵ R. N. Cahn,⁵ R. G. Jacobsen,⁵ L. T. Kerth,⁵ Yu. G. Kolomensky,⁵
G. Kukartsev,⁵ G. Lynch,⁵ I. L. Osipenkov,⁵ M. T. Ronan,^{5,*} K. Tackmann,⁵ T. Tanabe,⁵ C. M. Hawkes,⁶ N. Soni,⁶
A. T. Watson,⁶ H. Koch,⁷ T. Schroeder,⁷ D. Walker,⁸ D. J. Asgeirsson,⁹ T. Cuhadar-Donszelmann,⁹ B. G. Fulson,⁹
C. Hearty,⁹ T. S. Mattison,⁹ J. A. McKenna,⁹ M. Barrett,¹⁰ A. Khan,¹⁰ L. Teodorescu,¹⁰ V. E. Blinov,¹¹
A. D. Bukin,¹¹ A. R. Buzykaev,¹¹ V. P. Druzhinin,¹¹ V. B. Golubev,¹¹ A. P. Onuchin,¹¹ S. I. Serebnyakov,¹¹
Yu. I. Skovpen,¹¹ E. P. Solodov,¹¹ K. Yu. Todyshev,¹¹ M. Bondioli,¹² S. Curry,¹² I. Eschrich,¹² D. Kirkby,¹²
A. J. Lankford,¹² P. Lund,¹² M. Mandelkern,¹² E. C. Martin,¹² D. P. Stoker,¹² S. Abachi,¹³ C. Buchanan,¹³
J. W. Gary,¹⁴ F. Liu,¹⁴ O. Long,¹⁴ B. C. Shen,^{14,*} G. M. Vitug,¹⁴ Z. Yasin,¹⁴ L. Zhang,¹⁴ V. Sharma,¹⁵
C. Campagnari,¹⁶ T. M. Hong,¹⁶ D. Kovalskiy,¹⁶ M. A. Mazur,¹⁶ J. D. Richman,¹⁶ T. W. Beck,¹⁷ A. M. Eisner,¹⁷
C. J. Flacco,¹⁷ C. A. Heusch,¹⁷ J. Kroseberg,¹⁷ W. S. Lockman,¹⁷ T. Schalk,¹⁷ B. A. Schumm,¹⁷ A. Seiden,¹⁷
L. Wang,¹⁷ M. G. Wilson,¹⁷ L. O. Winstrom,¹⁷ C. H. Cheng,¹⁸ D. A. Doll,¹⁸ B. Echenard,¹⁸ F. Fang,¹⁸
D. G. Hitlin,¹⁸ I. Narsky,¹⁸ T. Piatenko,¹⁸ F. C. Porter,¹⁸ R. Andreassen,¹⁹ G. Mancinelli,¹⁹ B. T. Meadows,¹⁹
K. Mishra,¹⁹ M. D. Sokoloff,¹⁹ F. Blanc,²⁰ P. C. Bloom,²⁰ W. T. Ford,²⁰ A. Gaz,²⁰ J. F. Hirschauer,²⁰ A. Kreisel,²⁰
M. Nagel,²⁰ U. Nauenberg,²⁰ J. G. Smith,²⁰ K. A. Ulmer,²⁰ S. R. Wagner,²⁰ R. Ayad,^{21,†} A. Soffer,^{21,‡}
W. H. Toki,²¹ R. J. Wilson,²¹ D. D. Altenburg,²² E. Feltresi,²² A. Hauke,²² H. Jasper,²² M. Karbach,²² J. Merkel,²²
A. Petzold,²² B. Spaan,²² K. Wacker,²² M. J. Kobel,²³ W. F. Mader,²³ R. Nogowski,²³ K. R. Schubert,²³
R. Schwierz,²³ J. E. Sundermann,²³ A. Volk,²³ D. Bernard,²⁴ G. R. Bonneaud,²⁴ E. Latour,²⁴ Ch. Thiebaux,²⁴
M. Verderi,²⁴ P. J. Clark,²⁵ W. Gradl,²⁵ S. Playfer,²⁵ J. E. Watson,²⁵ M. Andreotti^{ab,26}, D. Bettoni^{a,26}, C. Bozzi^{a,26},
R. Calabrese^{ab,26}, A. Cecchi^{ab,26}, G. Cibinetto^{ab,26}, P. Franchini^{ab,26}, E. Luppi^{ab,26}, M. Negrini^{ab,26}, A. Petrella^{ab,26},
L. Piemontese^{a,26}, V. Santoro^{ab,26}, R. Baldini-Ferrolli,²⁷ A. Calcaterra,²⁷ R. de Sangro,²⁷ G. Finocchiaro,²⁷
S. Pacetti,²⁷ P. Patteri,²⁷ I. M. Peruzzi,^{27,§} M. Piccolo,²⁷ M. Rama,²⁷ A. Zallo,²⁷ A. Buzzo^{a,28}, R. Contri^{ab,28},
M. Lo Vetere^{ab,28}, M. M. Macri^{a,28}, M. R. Monge^{ab,28}, S. Passaggio^{a,28}, C. Patrignani^{ab,28}, E. Robutti^{a,28},
A. Santroni^{ab,28}, S. Tosi^{ab,28}, K. S. Chaisanguanthum,²⁹ M. Morii,²⁹ R. S. Dubitzky,³⁰ J. Marks,³⁰ S. Schenk,³⁰
U. Uwer,³⁰ V. Klose,³¹ H. M. Lacker,³¹ G. De Nardo^{ab,32}, L. Lista^{a,32}, D. Monorchio^{ab,32}, G. Onorato^{ab,32},
C. Sciacca^{ab,32}, D. J. Bard,³³ P. D. Dauncey,³³ J. A. Nash,³³ W. Panduro Vazquez,³³ M. Tibbetts,³³ P. K. Behera,³⁴
X. Chai,³⁴ M. J. Charles,³⁴ U. Mallik,³⁴ J. Cochran,³⁵ H. B. Crawley,³⁵ L. Dong,³⁵ W. T. Meyer,³⁵ S. Prell,³⁵
E. I. Rosenberg,³⁵ A. E. Rubin,³⁵ Y. Y. Gao,³⁶ A. V. Gritsan,³⁶ Z. J. Guo,³⁶ C. K. Lae,³⁶ A. G. Denig,³⁷
M. Fritsch,³⁷ G. Schott,³⁷ N. Arnaud,³⁸ J. Béquilleux,³⁸ A. D’Orazio,³⁸ M. Davier,³⁸ J. Firmino da Costa,³⁸
G. Grosdidier,³⁸ A. Höcker,³⁸ V. Lepeltier,³⁸ F. Le Diberder,³⁸ A. M. Lutz,³⁸ S. Pruvot,³⁸ P. Roudeau,³⁸
M. H. Schune,³⁸ J. Serrano,³⁸ V. Sordini,^{38,¶} A. Stocchi,³⁸ G. Wormser,³⁸ D. J. Lange,³⁹ D. M. Wright,³⁹
I. Bingham,⁴⁰ J. P. Burke,⁴⁰ C. A. Chavez,⁴⁰ J. R. Fry,⁴⁰ E. Gabathuler,⁴⁰ R. Gamet,⁴⁰ D. E. Hutchcroft,⁴⁰
D. J. Payne,⁴⁰ C. Touramanis,⁴⁰ A. J. Bevan,⁴¹ K. A. George,⁴¹ F. Di Lodovico,⁴¹ R. Sacco,⁴¹ M. Sigamani,⁴¹
G. Cowan,⁴² H. U. Flaecher,⁴² D. A. Hopkins,⁴² S. Paramesvaran,⁴² F. Salvatore,⁴² A. C. Wren,⁴² D. N. Brown,⁴³
C. L. Davis,⁴³ K. E. Alwyn,⁴⁴ N. R. Barlow,⁴⁴ R. J. Barlow,⁴⁴ Y. M. Chia,⁴⁴ C. L. Edgar,⁴⁴ G. D. Lafferty,⁴⁴
T. J. West,⁴⁴ J. I. Yi,⁴⁴ J. Anderson,⁴⁵ C. Chen,⁴⁵ A. Jawahery,⁴⁵ D. A. Roberts,⁴⁵ G. Simi,⁴⁵ J. M. Tuggle,⁴⁵
C. Dallapiccola,⁴⁶ S. S. Hertzbach,⁴⁶ X. Li,⁴⁶ E. Salvati,⁴⁶ S. Saremi,⁴⁶ R. Cowan,⁴⁷ D. Dujmic,⁴⁷
P. H. Fisher,⁴⁷ K. Koeneke,⁴⁷ G. Sciolla,⁴⁷ M. Spitznagel,⁴⁷ F. Taylor,⁴⁷ R. K. Yamamoto,⁴⁷ M. Zhao,⁴⁷
S. E. Mclachlin,^{48,*} P. M. Patel,⁴⁸ S. H. Robertson,⁴⁸ A. Lazzaro^{ab,49}, V. Lombardo^{a,49}, F. Palombo^{ab,49},
J. M. Bauer,⁵⁰ L. Cremaldi,⁵⁰ V. Eschenburg,⁵⁰ R. Godang,^{50,**} R. Kroeger,⁵⁰ D. A. Sanders,⁵⁰ D. J. Summers,⁵⁰
H. W. Zhao,⁵⁰ M. Simard,⁵¹ P. Taras,⁵¹ F. B. Viaud,⁵¹ H. Nicholson,⁵² M. A. Baak,⁵³ G. Raven,⁵³ H. L. Snoek,⁵³
C. P. Jessop,⁵⁴ K. J. Knoepfel,⁵⁴ J. M. LoSecco,⁵⁴ W. F. Wang,⁵⁴ G. Benelli,⁵⁵ L. A. Corwin,⁵⁵ K. Honscheid,⁵⁵
H. Kagan,⁵⁵ R. Kass,⁵⁵ J. P. Morris,⁵⁵ A. M. Rahimi,⁵⁵ J. J. Regensburger,⁵⁵ S. J. Sekula,⁵⁵ Q. K. Wong,⁵⁵
N. L. Blount,⁵⁶ J. Brau,⁵⁶ R. Frey,⁵⁶ O. Igonkina,⁵⁶ J. A. Kolb,⁵⁶ M. Lu,⁵⁶ R. Rahmat,⁵⁶ N. B. Sinev,⁵⁶ D. Strom,⁵⁶
J. Strube,⁵⁶ E. Torrence,⁵⁶ G. Castelli^{ab,57}, N. Gagliardi^{ab,57}, M. Margoni^{ab,57}, M. Morandin^{a,57}, M. Posocco^{a,57}

M. Rotondo^{a,57} F. Simonetto^{ab,57} R. Stroili^{ab,57} C. Voci^{ab,57} P. del Amo Sanchez,⁵⁸ E. Ben-Haim,⁵⁸ H. Briand,⁵⁸ G. Calderini,⁵⁸ J. Chauveau,⁵⁸ P. David,⁵⁸ L. Del Buono,⁵⁸ O. Hamon,⁵⁸ Ph. Leruste,⁵⁸ J. Ocariz,⁵⁸ A. Perez,⁵⁸ J. Prendki,⁵⁸ L. Gladney,⁵⁹ M. Biasini^{ab,60} R. Covarelli^{ab,60} E. Manoni^{ab,60} C. Angelini^{ab,61} G. Batignani^{ab,61} S. Bettarini^{ab,61} M. Carpinelli^{ab,61,††} A. Cervelli^{ab,61} F. Forti^{ab,61} M. A. Giorgi^{ab,61} A. Lusiani^{ac,61} G. Marchiori^{ab,61} M. Morganti^{ab,61} N. Neri^{ab,61} E. Paoloni^{ab,61} G. Rizzo^{ab,61} J. J. Walsh^{a,61} J. Biesiada,⁶² D. Lopes Pegna,⁶² C. Lu,⁶² J. Olsen,⁶² A. J. S. Smith,⁶² A. V. Telnov,⁶² F. Anulli^{a,63} E. Baracchini^{ab,63} G. Cavoto^{a,63} D. del Re^{ab,63} E. Di Marco^{ab,63} R. Faccini^{ab,63} F. Ferrarotto^{a,63} F. Ferroni^{ab,63} M. Gaspero^{ab,63} P. D. Jackson^{a,63} L. Li Gioi^{a,63} M. A. Mazzoni^{a,63} S. Morganti^{a,63} G. Piredda^{a,63} F. Polci^{ab,63} F. Renga^{ab,63} C. Voena^{a,63} M. Ebert,⁶⁴ T. Hartmann,⁶⁴ H. Schröder,⁶⁴ R. Waldi,⁶⁴ T. Adye,⁶⁵ B. Franek,⁶⁵ E. O. Olaiya,⁶⁵ W. Roethel,⁶⁵ F. F. Wilson,⁶⁵ S. Emery,⁶⁶ M. Escalier,⁶⁶ L. Esteve,⁶⁶ A. Gaidot,⁶⁶ S. F. Ganzhur,⁶⁶ G. Hamel de Monchenault,⁶⁶ W. Kozanecki,⁶⁶ G. Vasseur,⁶⁶ Ch. Yèche,⁶⁶ M. Zito,⁶⁶ X. R. Chen,⁶⁷ H. Liu,⁶⁷ W. Park,⁶⁷ M. V. Purohit,⁶⁷ R. M. White,⁶⁷ J. R. Wilson,⁶⁷ M. T. Allen,⁶⁸ D. Aston,⁶⁸ R. Bartoldus,⁶⁸ P. Bechtel,⁶⁸ J. F. Benitez,⁶⁸ R. Cenci,⁶⁸ J. P. Coleman,⁶⁸ M. R. Convery,⁶⁸ J. C. Dingfelder,⁶⁸ J. Dorfan,⁶⁸ G. P. Dubois-Felsmann,⁶⁸ W. Dunwoodie,⁶⁸ R. C. Field,⁶⁸ A. M. Gabareen,⁶⁸ S. J. Gowdy,⁶⁸ M. T. Graham,⁶⁸ P. Grenier,⁶⁸ C. Hast,⁶⁸ W. R. Innes,⁶⁸ J. Kaminski,⁶⁸ M. H. Kelsey,⁶⁸ H. Kim,⁶⁸ P. Kim,⁶⁸ M. L. Kocian,⁶⁸ D. W. G. S. Leith,⁶⁸ S. Li,⁶⁸ B. Lindquist,⁶⁸ S. Luitz,⁶⁸ V. Luth,⁶⁸ H. L. Lynch,⁶⁸ D. B. MacFarlane,⁶⁸ H. Marsiske,⁶⁸ R. Messner,⁶⁸ D. R. Muller,⁶⁸ H. Neal,⁶⁸ S. Nelson,⁶⁸ C. P. O'Grady,⁶⁸ I. Ofte,⁶⁸ A. Perazzo,⁶⁸ M. Perl,⁶⁸ B. N. Ratcliff,⁶⁸ A. Roodman,⁶⁸ A. A. Salnikov,⁶⁸ R. H. Schindler,⁶⁸ J. Schwiening,⁶⁸ A. Snyder,⁶⁸ D. Su,⁶⁸ M. K. Sullivan,⁶⁸ K. Suzuki,⁶⁸ S. K. Swain,⁶⁸ J. M. Thompson,⁶⁸ J. Va'vra,⁶⁸ A. P. Wagner,⁶⁸ M. Weaver,⁶⁸ C. A. West,⁶⁸ W. J. Wisniewski,⁶⁸ M. Wittgen,⁶⁸ D. H. Wright,⁶⁸ H. W. Wulsin,⁶⁸ A. K. Yarritu,⁶⁸ K. Yi,⁶⁸ C. C. Young,⁶⁸ V. Ziegler,⁶⁸ P. R. Burchat,⁶⁹ A. J. Edwards,⁶⁹ S. A. Majewski,⁶⁹ T. S. Miyashita,⁶⁹ B. A. Petersen,⁶⁹ L. Wilden,⁶⁹ S. Ahmed,⁷⁰ M. S. Alam,⁷⁰ R. Bula,⁷⁰ J. A. Ernst,⁷⁰ B. Pan,⁷⁰ M. A. Saeed,⁷⁰ S. B. Zain,⁷⁰ S. M. Spanier,⁷¹ B. J. Wogslund,⁷¹ R. Eckmann,⁷² J. L. Ritchie,⁷² A. M. Ruland,⁷² C. J. Schilling,⁷² R. F. Schwitters,⁷² B. W. Drummond,⁷³ J. M. Izen,⁷³ X. C. Lou,⁷³ F. Bianchi^{ab,74} D. Gamba^{ab,74} M. Pelliccioni^{ab,74} M. Bomben^{ab,75} L. Bosisio^{ab,75} C. Cartaro^{ab,75} G. Della Ricca^{ab,75} L. Lanceri^{ab,75} L. Vitale^{ab,75} V. Azzolini,⁷⁶ N. Lopez-March,⁷⁶ F. Martinez-Vidal,⁷⁶ D. A. Milanes,⁷⁶ A. Oyanguren,⁷⁶ J. Albert,⁷⁷ Sw. Banerjee,⁷⁷ B. Bhuyan,⁷⁷ H. H. F. Choi,⁷⁷ K. Hamano,⁷⁷ R. Kowalewski,⁷⁷ M. J. Lewczuk,⁷⁷ I. M. Nugent,⁷⁷ J. M. Roney,⁷⁷ R. J. Sobie,⁷⁷ T. J. Gershon,⁷⁸ P. F. Harrison,⁷⁸ J. Ilic,⁷⁸ T. E. Latham,⁷⁸ G. B. Mohanty,⁷⁸ H. R. Band,⁷⁹ X. Chen,⁷⁹ S. Dasu,⁷⁹ K. T. Flood,⁷⁹ Y. Pan,⁷⁹ M. Pierini,⁷⁹ R. Prepost,⁷⁹ C. O. Vuosalo,⁷⁹ and S. L. Wu⁷⁹

(The BABAR Collaboration)

¹Laboratoire de Physique des Particules, IN2P3/CNRS et Université de Savoie, F-74941 Annecy-Le-Vieux, France

²Universitat de Barcelona, Facultat de Física, Departament ECM, E-08028 Barcelona, Spain

³INFN Sezione di Bari^a; Dipartimento di Fisica, Università di Bari^b, I-70126 Bari, Italy

⁴University of Bergen, Institute of Physics, N-5007 Bergen, Norway

⁵Lawrence Berkeley National Laboratory and University of California, Berkeley, California 94720, USA

⁶University of Birmingham, Birmingham, B15 2TT, United Kingdom

⁷Ruhr Universität Bochum, Institut für Experimentalphysik 1, D-44780 Bochum, Germany

⁸University of Bristol, Bristol BS8 1TL, United Kingdom

⁹University of British Columbia, Vancouver, British Columbia, Canada V6T 1Z1

¹⁰Brunel University, Uxbridge, Middlesex UB8 3PH, United Kingdom

¹¹Budker Institute of Nuclear Physics, Novosibirsk 630090, Russia

¹²University of California at Irvine, Irvine, California 92697, USA

¹³University of California at Los Angeles, Los Angeles, California 90024, USA

¹⁴University of California at Riverside, Riverside, California 92521, USA

¹⁵University of California at San Diego, La Jolla, California 92093, USA

¹⁶University of California at Santa Barbara, Santa Barbara, California 93106, USA

¹⁷University of California at Santa Cruz, Institute for Particle Physics, Santa Cruz, California 95064, USA

¹⁸California Institute of Technology, Pasadena, California 91125, USA

¹⁹University of Cincinnati, Cincinnati, Ohio 45221, USA

²⁰University of Colorado, Boulder, Colorado 80309, USA

²¹Colorado State University, Fort Collins, Colorado 80523, USA

²²Technische Universität Dortmund, Fakultät Physik, D-44221 Dortmund, Germany

²³Technische Universität Dresden, Institut für Kern- und Teilchenphysik, D-01062 Dresden, Germany

²⁴Laboratoire Leprince-Ringuet, CNRS/IN2P3, Ecole Polytechnique, F-91128 Palaiseau, France

²⁵University of Edinburgh, Edinburgh EH9 3JZ, United Kingdom

²⁶INFN Sezione di Ferrara^a; Dipartimento di Fisica, Università di Ferrara^b, I-44100 Ferrara, Italy

- ²⁷INFN Laboratori Nazionali di Frascati, I-00044 Frascati, Italy
- ²⁸INFN Sezione di Genova^a; Dipartimento di Fisica, Università di Genova^b, I-16146 Genova, Italy
- ²⁹Harvard University, Cambridge, Massachusetts 02138, USA
- ³⁰Universität Heidelberg, Physikalisches Institut, Philosophenweg 12, D-69120 Heidelberg, Germany
- ³¹Humboldt-Universität zu Berlin, Institut für Physik, Newtonstr. 15, D-12489 Berlin, Germany
- ³²INFN Sezione di Napoli^a; Dipartimento di Scienze Fisiche, Università di Napoli Federico II^b, I-80126 Napoli, Italy
- ³³Imperial College London, London, SW7 2AZ, United Kingdom
- ³⁴University of Iowa, Iowa City, Iowa 52242, USA
- ³⁵Iowa State University, Ames, Iowa 50011-3160, USA
- ³⁶Johns Hopkins University, Baltimore, Maryland 21218, USA
- ³⁷Universität Karlsruhe, Institut für Experimentelle Kernphysik, D-76021 Karlsruhe, Germany
- ³⁸Laboratoire de l'Accélérateur Linéaire, IN2P3/CNRS et Université Paris-Sud 11, Centre Scientifique d'Orsay, B. P. 34, F-91898 ORSAY Cedex, France
- ³⁹Lawrence Livermore National Laboratory, Livermore, California 94550, USA
- ⁴⁰University of Liverpool, Liverpool L69 7ZE, United Kingdom
- ⁴¹Queen Mary, University of London, E1 4NS, United Kingdom
- ⁴²University of London, Royal Holloway and Bedford New College, Egham, Surrey TW20 0EX, United Kingdom
- ⁴³University of Louisville, Louisville, Kentucky 40292, USA
- ⁴⁴University of Manchester, Manchester M13 9PL, United Kingdom
- ⁴⁵University of Maryland, College Park, Maryland 20742, USA
- ⁴⁶University of Massachusetts, Amherst, Massachusetts 01003, USA
- ⁴⁷Massachusetts Institute of Technology, Laboratory for Nuclear Science, Cambridge, Massachusetts 02139, USA
- ⁴⁸McGill University, Montréal, Québec, Canada H3A 2T8
- ⁴⁹INFN Sezione di Milano^a; Dipartimento di Fisica, Università di Milano^b, I-20133 Milano, Italy
- ⁵⁰University of Mississippi, University, Mississippi 38677, USA
- ⁵¹Université de Montréal, Physique des Particules, Montréal, Québec, Canada H3C 3J7
- ⁵²Mount Holyoke College, South Hadley, Massachusetts 01075, USA
- ⁵³NIKHEF, National Institute for Nuclear Physics and High Energy Physics, NL-1009 DB Amsterdam, The Netherlands
- ⁵⁴University of Notre Dame, Notre Dame, Indiana 46556, USA
- ⁵⁵Ohio State University, Columbus, Ohio 43210, USA
- ⁵⁶University of Oregon, Eugene, Oregon 97403, USA
- ⁵⁷INFN Sezione di Padova^a; Dipartimento di Fisica, Università di Padova^b, I-35131 Padova, Italy
- ⁵⁸Laboratoire de Physique Nucléaire et de Hautes Energies, IN2P3/CNRS, Université Pierre et Marie Curie-Paris6, Université Denis Diderot-Paris7, F-75252 Paris, France
- ⁵⁹University of Pennsylvania, Philadelphia, Pennsylvania 19104, USA
- ⁶⁰INFN Sezione di Perugia^a; Dipartimento di Fisica, Università di Perugia^b, I-06100 Perugia, Italy
- ⁶¹INFN Sezione di Pisa^a; Dipartimento di Fisica, Università di Pisa^b; Scuola Normale Superiore di Pisa^c, I-56127 Pisa, Italy
- ⁶²Princeton University, Princeton, New Jersey 08544, USA
- ⁶³INFN Sezione di Roma^a; Dipartimento di Fisica, Università di Roma La Sapienza^b, I-00185 Roma, Italy
- ⁶⁴Universität Rostock, D-18051 Rostock, Germany
- ⁶⁵Rutherford Appleton Laboratory, Chilton, Didcot, Oxon, OX11 0QX, United Kingdom
- ⁶⁶DSM/Dapnia, CEA/Saclay, F-91191 Gif-sur-Yvette, France
- ⁶⁷University of South Carolina, Columbia, South Carolina 29208, USA
- ⁶⁸Stanford Linear Accelerator Center, Stanford, California 94309, USA
- ⁶⁹Stanford University, Stanford, California 94305-4060, USA
- ⁷⁰State University of New York, Albany, New York 12222, USA
- ⁷¹University of Tennessee, Knoxville, Tennessee 37996, USA
- ⁷²University of Texas at Austin, Austin, Texas 78712, USA
- ⁷³University of Texas at Dallas, Richardson, Texas 75083, USA
- ⁷⁴INFN Sezione di Torino^a; Dipartimento di Fisica Sperimentale, Università di Torino^b, I-10125 Torino, Italy
- ⁷⁵INFN Sezione di Trieste^a; Dipartimento di Fisica, Università di Trieste^b, I-34127 Trieste, Italy
- ⁷⁶IFIC, Universitat de Valencia-CSIC, E-46071 Valencia, Spain
- ⁷⁷University of Victoria, Victoria, British Columbia, Canada V8W 3P6
- ⁷⁸Department of Physics, University of Warwick, Coventry CV4 7AL, United Kingdom
- ⁷⁹University of Wisconsin, Madison, Wisconsin 53706, USA

(Dated: November 9, 2018)

Using 214 fb⁻¹ of data recorded by the BABAR detector at the PEP-II electron-positron collider, we study the decay $D_s^+ \rightarrow K^+ K^- e^+ \nu_e$. Except for a small S-wave contribution, the events with $K^+ K^-$ masses in the range 1.01-1.03 GeV/c² correspond to ϕ mesons. For $D_s^+ \rightarrow \phi e^+ \nu_e$ decays, we measure

the relative normalization of the Lorentz invariant form factors at $q^2 = 0$, $r_V = V(0)/A_1(0) = 1.849 \pm 0.060 \pm 0.095$, $r_2 = A_2(0)/A_1(0) = 0.763 \pm 0.071 \pm 0.065$ and the pole mass of the axial-vector form factors $m_A = (2.28_{-0.18}^{+0.23} \pm 0.18)$ GeV/ c^2 . Within the same K^+K^- mass range, we also measure the relative branching fraction $\mathcal{B}(D_s^+ \rightarrow K^+K^-e^+\nu_e)/\mathcal{B}(D_s^+ \rightarrow K^+K^-\pi^+) = 0.558 \pm 0.007 \pm 0.016$, from which we obtain the total branching fraction $\mathcal{B}(D_s^+ \rightarrow \phi e^+\nu_e) = (2.61 \pm 0.03 \pm 0.08 \pm 0.15) \times 10^{-2}$. By comparing this value with the predicted decay rate, we extract $A_1(0) = 0.607 \pm 0.011 \pm 0.019 \pm 0.018$. The stated uncertainties are statistical, systematic, and from external inputs.

PACS numbers: 12.15.Hh, 12.38.Gc, 13.20.Fc, 14.40.Lb

Charm semileptonic decays can help to validate predictions from lattice QCD through precise measurements of hadronic form factors. Such measurements have been performed by BABAR for the $D^0 \rightarrow K^-e^+\nu_e$ decays [1]. The $D_s^+ \rightarrow \phi e^+\nu_e$ [2] channel is well suited to study form factors in semileptonic decays of charm mesons to a vector particle because the ϕ meson is a narrow resonance which can be well isolated experimentally. Because of the higher mass of the spectator s -quark, form factor determinations for this process by lattice QCD are expected to be more accurate than for non-strange D mesons. However, measurements of this decay mode are impacted by the lower production rate for D_s^+ mesons and higher backgrounds. Form factors in $D_s^+ \rightarrow \phi e^+\nu_e$ have been previously studied by photoproduction experiments, at Fermilab [3, 4, 5, 6], and by CLEOII at the CESR e^+e^- collider also operating at the $\Upsilon(4S)$ [7]. In charm meson semileptonic decays, a ϕ meson is expected to originate only from the D_s^+ . A possible contribution from the Cabibbo suppressed $D^+ \rightarrow \phi e^+\nu_e$ decay, through the $d\bar{d}$ component of the ϕ meson [8] is neglected [9].

Using 214 fb $^{-1}$ of data collected at the $\Upsilon(4S)$ resonance by the BABAR detector, we measure the $D_s^+ \rightarrow K^+K^-e^+\nu_e$ channel decay characteristics, for events produced in the continuum $e^+e^- \rightarrow c\bar{c}$. The analysis focuses on the $\phi e^+\nu_e$ final state in the K^+K^- invariant mass range between 1.01 and 1.03 GeV/ c^2 . The ϕ resonance is dominant in this K^+K^- invariant mass region although a small S-wave component is observed, for the first time, through its interference with the ϕ .

The differential decay rate for $D_s^+ \rightarrow K^+K^-e^+\nu_e$ depends on five variables [10]: m_{KK}^2 , the mass squared of the K^+K^- system; q^2 , the mass squared of the $e^+\nu_e$ system; $\cos\theta_e$ ($\cos\theta_K$), where θ_e (θ_K) is the angle between the momentum of the e^+ (K^+) in the $e^+\nu_e$ (K^+K^-) rest frame and the momentum of the $e^+\nu_e$ (K^+K^-) system in the D_s^+ rest frame; and χ , the angle between the normals to the planes defined in the D_s^+ rest frame by the K^+K^- pair and the $e^+\nu_e$ pair. When analyzing a D_s^- candidate, the direction of the K^- is used in place of the K^+ and χ is changed to $-\chi$. The expression for the differential decay rate as a function of these variables is given in ref. [11]. Neglecting contributions proportional to the square of the electron mass, it depends on three hadronic form factors which are related to the three possible helicity values of the hadronic current. Restricting

to S- and P-wave contributions, these form factors can be written as:

$$\mathcal{F}_1 = \mathcal{F}_{10} + \mathcal{F}_{11} \cos\theta_K, \quad \mathcal{F}_2 = \frac{1}{\sqrt{2}}\mathcal{F}_{21}, \quad \mathcal{F}_3 = \frac{1}{\sqrt{2}}\mathcal{F}_{31}. \quad (1)$$

The form factors \mathcal{F}_{ij} depend only on m_{KK}^2 and q^2 ; \mathcal{F}_{10} characterizes the S-wave contribution, whereas the \mathcal{F}_{i1} correspond to the ϕ meson:

$$\mathcal{F}_{i1} = \sqrt{3}\pi q H_i(q^2, m) \mathcal{A}_\phi(m), \quad (2)$$

where the ϕ meson decay amplitude $\mathcal{A}_\phi(m)$ is taken to be a relativistic Breit-Wigner distribution with a mass-dependent width including a Blatt-Weisskopf damping factor [12]. The form factors $H_{1,2,3}$ can be expressed in terms of the Lorentz invariant form factors V and $A_{1,2}$ [13], for which we assume a q^2 dependence dominated by a single pole:

$$V(q^2) = \frac{V(0)}{1 - q^2/m_V^2}; \quad A_{1,2}(q^2) = \frac{A_{1,2}(0)}{1 - q^2/m_A^2}. \quad (3)$$

m_A and m_V are the pole masses, usually fixed to the values of corresponding resonance masses: $m_A = 2.5$ GeV/ c^2 ($\simeq m_{D_{s1}}$) and $m_V = 2.1$ GeV/ c^2 ($\simeq m_{D_s^*}$). At $q^2 = 0$, the ratios of the form factors V and A_2 relative to A_1 are denoted by r_V and r_2 , respectively. The S-wave contribution is parameterized assuming f_0 production:

$$\mathcal{F}_{10} = r_0 \frac{p_{KK} m_{D_s}}{1 - \frac{q^2}{m_A^2}} \frac{m_{f_0} g_\pi}{m_{f_0}^2 - m^2 - im_{f_0} \Gamma_{f_0}^0}, \quad (4)$$

where r_0 is a normalization factor and p_{KK} is the magnitude of the three-momentum of the K^+K^- system in the D_s^+ rest frame. The values of the f_0 parameters (m_{f_0} , g_π , $\Gamma_{f_0}^0$) are taken from Ref. [14].

A detailed description of the detector and the algorithms used for charged and neutral particle reconstruction and identification is provided elsewhere [15]. Monte Carlo (MC) samples of $\Upsilon(4S)$ decays, charm and other light quarks pairs from continuum events are generated using a GEANT4 [16]. Quark fragmentation, in continuum events, is described using the JETSET package [17]. Signal MC events are generated with seven times the equivalent statistics of the data, using a simple pole model for the form factors with $m_A = 2.5$ GeV/ c^2 and $m_V = 2.1$ GeV/ c^2 . The simulation of the characteristics of D_s^+ production is corrected to account for measured

differences compared to data. Radiative processes are simulated with PHOTOS [18].

We reconstruct $D_s^+ \rightarrow K^+K^-e^+\nu_e$ decays, for D_s^+ produced in $e^+e^- \rightarrow c\bar{c}$ events. The hadronization of the $c\bar{c}$ system leads to the formation of two jets, emitted back-to-back in the center-of-mass (c.m.) frame. The analysis method is similar to the one used for the decay $D^0 \rightarrow K^-e^+\nu_e$ [1]. The only differences are that the cascade from a D^* is not used to evaluate the signal, and the detector performance for the D_s^+ reconstruction is measured using $D_s^+ \rightarrow \phi\pi^+$ decays rather than the cascade decay $D^{*+} \rightarrow D^0\pi^+$, $D^0 \rightarrow K^-\pi^+$.

The event thrust axis is determined from all charged and neutral particles in the c.m. system and its direction is required to be in the range $|\cos(\theta_{\text{thrust}})| < 0.6$ to minimize the loss of particles in regions close to the beam axis. A plane perpendicular to the thrust axis is used to define two hemispheres, equivalent to the two jets produced by quark fragmentation. In each hemisphere, we search for the decay products of the D_s^+ , namely a positron, of momentum greater than $0.5 \text{ GeV}/c$, and two oppositely charged kaons. Since the ν_e momentum is unmeasured, a kinematic fit is performed, constraining the invariant mass of the candidate $K^+K^-e^+\nu_e$ system to the D_s^+ mass. In this fit, the D_s^+ direction and the neutrino energy are estimated from the other, charged and neutral, particles measured in the event. The D_s^+ direction is taken as the direction opposite to the sum of the momenta of all reconstructed particles, except for the kaons and the positron associated with the signal candidate. The neutrino energy is estimated as the difference between the total energy of the jet containing the candidate and the sum of the energies of all reconstructed particles in that hemisphere. The D_s^+ candidate is retained if the χ^2 probability of the kinematic fit exceeds 10^{-2} .

Sizable backgrounds arise from $\Upsilon(4S) \rightarrow B\bar{B}$ decays and two-jet events from $e^+e^- \rightarrow q\bar{q}$, $q = u, d, s, c$. Backgrounds are predominantly rejected by using two Fisher discriminant variables that exploit differences in the production characteristics of hadrons in signal and background. The first variable is used to separate signal in jet-like $c\bar{c}$ events from $B\bar{B}$ with a more spherical topology. The chosen cut retains 71% of the signal and rejects 86% of the $B\bar{B}$ background. The second Fisher discriminant uses variables related to the different production characteristics of particles from D_s decays and c -quark fragmentation. The selected cut retains 71% of the signal decays, and rejects 72% of the background. The overall signal efficiency is approximately 4.5%. Figure 1a) shows the K^+K^- invariant mass distribution for the selected decays compared to the simulation. There are 31,839 events in the signal region, with an estimated background of 20.3%. About 70% of the total background is peaking, corresponding to a ϕ decay combined with an electron from another source. The interference between S- and P-

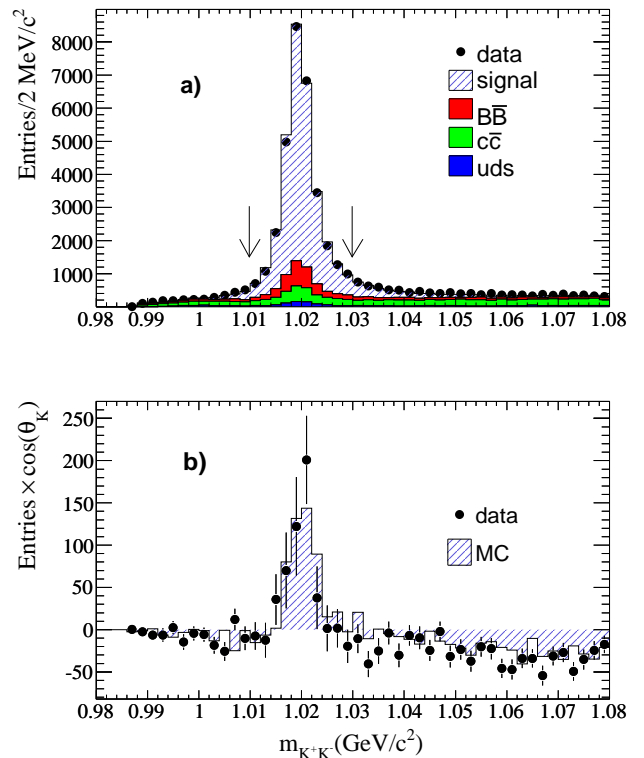


FIG. 1: a) K^+K^- invariant mass distribution from data and simulated events. MC events have been normalized to the data luminosity according to the different cross sections. The arrows indicate the selected K^+K^- mass interval. In b), each event is weighted by the measured value of $\cos\theta_K$. Negative entries are produced by the $c\bar{c}$ background asymmetry in $\cos\theta_K$.

waves generates an asymmetry in the $\cos\theta_K$ distribution which is revealed in Fig. 1b), where events have been weighted by $\cos\theta_K$.

To extract N_S (the number of reconstructed signal events), r_V , r_2 , m_A and r_0 , we perform a binned maximum likelihood fit to the four-dimensional decay distribution in the variables q^2 , $\cos\theta_e$, $\cos\theta_K$ and χ . The sensitivity to m_V is weak and we fix this parameter to $2.1 \text{ GeV}/c^2$. The data are divided into 625 bins, with five equal-sized bins per variable, and

$$\mathcal{L} = - \sum_{i=1}^{625} \ln \mathcal{P}(n_i^{\text{data}} | n_i^{\text{MC}}). \quad (5)$$

For each bin i , $\mathcal{P}(n_i^{\text{data}} | n_i^{\text{MC}})$ is the Poisson probability to observe n_i^{data} events when n_i^{MC} events are expected,

$$n_i^{\text{MC}}(\vec{\lambda}) = N_S \frac{\sum_{j=1}^{n_i^{\text{SMC}}} w_j(\vec{\lambda})}{W_{\text{tot}}(\vec{\lambda})} + n_i^{\text{BMC}}. \quad (6)$$

Here n_i^{SMC} is the number of signal MC events with re-

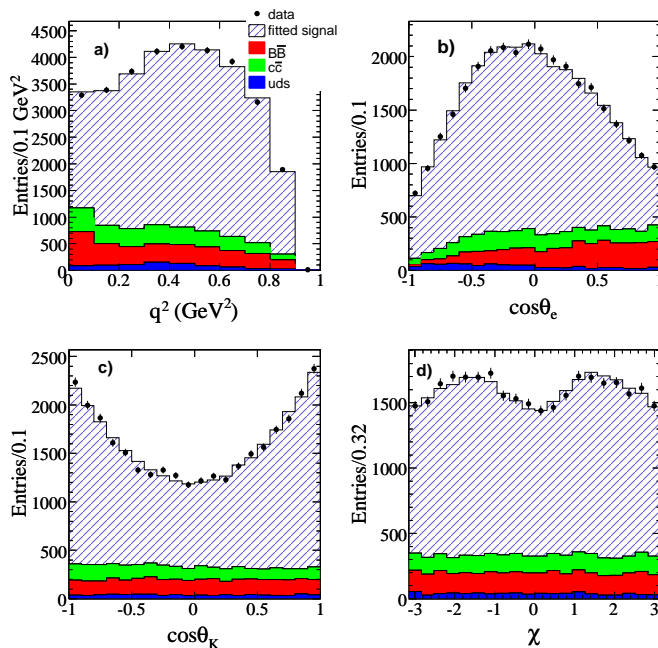


FIG. 2: Projected distributions of the reconstructed values of the four kinematic variables. The data (points with statistical uncertainties) are compared to the sum of four histograms, the fitted signal (light hatched) and the estimated background contributions (dark shaded).

constructed values of the four variables corresponding to bin i and n_i^{BMC} is the number of estimated background events. They are obtained from MC simulation, corrected for measured differences between data and simulation. Weights, w_j , are evaluated for each event, using the generated values of the kinematic variables, thus accounting for resolution effects. $W_{\text{tot}}(\vec{\lambda}) = \sum_{j=1}^{N^{\text{SMC}}} w_j(\vec{\lambda})$ is the sum of the weights for all simulated signal events (N^{SMC}) and $\vec{\lambda}$ corresponds to the parameters to be fitted. The data and results of the fit are shown in Fig. 2 and listed in Table I. From the fit we extract a contribution due to S-P wave interference. The value obtained for r_0 corresponds to a S-wave fraction of $(0.22^{+0.12}_{-0.08})\%$ of the decay rate.

In the fitting procedure, two sources of statistical fluctuations are not included. They originate from the finite sample of simulated signal events and the estimate of the average number of background events in each bin. These effects are evaluated with parameterized simulations and included in the systematic uncertainties. Other systematic effects have been assessed to account for the uncertainties in the c -quark hadronization, the background contributions, and the remaining uncertainties in the simulation of the detector response. They are summarized in Table I.

Corrections to the simulation of the c -quark fragmenta-

TABLE I: Measured values of the parameters N_S , r_V , r_2 , m_A (GeV/c^2), r_0 (GeV^{-1}), their statistical and systematic uncertainties.

	N_S	r_V	r_2	m_A	r_0
Fitted value	25341	1.849	0.763	2.28	15.1
Statistical uncertainty	178	0.060	0.071	$^{+0.23}_{-0.18}$	2.6
MC statistics	81	0.029	0.034	0.09	0.0
$c\bar{c}$ fragmentation	5	0.031	0.014	0.07	0.4
Background subtraction	480	0.081	0.049	0.14	0.6
Detector effects	12	0.021	0.021	0.07	0.6
Total syst. uncertainties	488	0.095	0.065	0.18	1.0

tion were performed iteratively, comparing variables used in the event selection for samples of $D_s^+ \rightarrow \phi\pi^+$ decays and applying a weight which depends on the values of these variables. We adopt the observed changes in the fit parameters for the last step in this iterative process as an estimate of the systematic uncertainty. Furthermore we assume a 30% uncertainty in the simulation of radiative effects.

The peaking and combinatorial background components from $e^+e^- \rightarrow c\bar{c}$ events have been studied separately. The peaking background contributions are studied by measuring inclusive ϕ production in events with a fully reconstructed D^{*+} or D_s^+ decay. The combinatorial background consists mainly of events with a charged lepton, one kaon from a D decay and a second kaon from fragmentation. We have measured the rate, momentum and angular distributions of K^\pm accompanying a D^0 , D^{*+} or D_s^+ meson in data and corrected the corresponding simulation.

After these corrections, the K^+K^- distribution for selected signal events in MC and data agree to within 10% above $1.03 \text{ GeV}/c^2$, and this remaining difference is adopted as the uncertainty in the normalization of the combinatorial background. The $B\bar{B}$ background is obtained from the difference of the data recorded at the $\Upsilon(4S)$ resonance and the data recorded $40 \text{ MeV}/c$ below. The related systematic uncertainties are obtained from the statistical accuracy of these measurements and from the uncertainty (0.25%) between the relative normalization of the two data samples. Systematic uncertainties also originate from the simulation of the detector response. There are small differences in the efficiencies for charged particle reconstruction and electron and kaon identification. They lead to data-MC differences in the reconstruction of the D_s^+ direction and the neutrino energy. They are estimated using $D_s^+ \rightarrow \phi\pi^+$ decays.

We measure the $D_s^+ \rightarrow K^+K^-e^+\nu_e$ branching fraction relative to the decay, $D_s^+ \rightarrow K^+K^-\pi^+$ for which we adopt the K^+K^- mass interval, $1.0095\text{-}1.0295 \text{ GeV}/c^2$, to match the range used by CLEO-c for the $D_s^+ \rightarrow K^+K^-\pi^+$ branching fraction measurement [19]. Specifically, we compare the ratio of rates for the two channels

in data and simulated events so that most systematic uncertainties cancel [1]. In the considered mass intervals, we obtain $R_{D_s} = \frac{\mathcal{B}(D_s^+ \rightarrow K^+ K^- e^+ \nu_e)}{\mathcal{B}(D_s^+ \rightarrow K^+ K^- \pi^+)} = 0.558 \pm 0.007 \pm 0.016$.

Systematic uncertainties are summarized in Table II. They originate mainly from selection criteria that are not common for the two channels. Differences in the impact of the two Fisher discriminants have been estimated by varying the selection cuts and differences in particle identification for electrons and pions are accounted for. The uncertainty on N_S is taken from the previous fit; it is dominated by uncertainties in the background evaluation. We translate the ratio R_{D_s} to a branching fraction,

TABLE II: Summary of the relative systematic uncertainties on R_{D_s} .

Source	Relative variation
Fisher variable against $c\bar{c}$ events	$\pm 1.77\%$
Fisher variable against $b\bar{b}$ events	$\pm 0.58\%$
Fitted signal (N_S)	$\pm 1.92\%$
PID corrections	$\pm 0.74\%$
D_s^+ production	$\pm 0.20\%$
Mass constrained fit	$\pm 0.61\%$
Total systematic uncertainty	$\pm 2.85\%$

using $\mathcal{B}(D_s^+ \rightarrow K^+ K^- \pi^+) = (1.99 \pm 0.10 \pm 0.05)\%$ [19], correcting for the finite mass range used to select signal events ($86.37 \pm 1.22\%$), subtracting the S-wave contribution, and taking $\mathcal{B}(\phi \rightarrow K^+ K^-) = (49.2 \pm 0.6)\%$ [8]. We find:

$$\mathcal{B}(D_s^+ \rightarrow \phi e^+ \nu_e) = (2.61 \pm 0.03 \pm 0.08 \pm 0.15) \times 10^{-2},$$

where the last quoted uncertainty corresponds to external inputs.

In conclusion, we have studied the decay $D_s^+ \rightarrow K^+ K^- e^+ \nu_e$ with a sample of approximately 25,000 signal events, which greatly exceeds any previous measurement. This decay is dominated by the ϕ vector meson; we measure a small S-wave contribution, possibly associated with $f_0 \rightarrow K^+ K^-$, corresponding to $(0.22_{-0.08}^{+0.12} \pm 0.03)\%$ of the $K^+ K^- e^+ \nu_e$ decay rate. We have extracted form factor parameters from a fit to the four-dimensional decay distribution, assuming single pole dominance and obtain: $r_V = V(0)/A_1(0) = 1.849 \pm 0.060 \pm 0.095$, $r_2 = A_2(0)/A_1(0) = 0.763 \pm 0.071 \pm 0.065$ and the pole mass of the axial-vector form factors $m_A = (2.28_{-0.18}^{+0.23} \pm 0.18)$ GeV/ c^2 . For comparison with previous measurements we also perform the fit to the data with fixed pole masses $m_A = 2.5$ GeV/ c^2 and $m_V = 2.1$ GeV/ c^2 , ignoring also the small S-wave contribution. The results on r_2 and r_V represent a large improvement in statistical and systematic precision compared to earlier measurements [3, 4, 5, 6, 7] (see Table III).

We also measure the relative branching fraction $\mathcal{B}(D_s^+ \rightarrow K^+ K^- e^+ \nu_e)/\mathcal{B}(D_s^+ \rightarrow K^+ K^- \pi^+) = 0.558 \pm$

TABLE III: Results from previous experiments and present measurements.

Experiment	r_V	r_2
E653 [3]	$2.3_{-0.9}^{+1.1} \pm 0.4$	$2.1_{-0.5}^{+0.6} \pm 0.2$
E687 [4]	$1.8 \pm 0.9 \pm 0.2$	$1.1 \pm 0.8 \pm 0.1$
E791 [5]	$2.27 \pm 0.35 \pm 0.22$	$1.57 \pm 0.25 \pm 0.19$
FOCUS [6]	$1.549 \pm 0.250 \pm 0.145$	$0.713 \pm 0.202 \pm 0.266$
CLEOII [7]	$0.9 \pm 0.6 \pm 0.3$	$1.4 \pm 0.5 \pm 0.3$
BABAR	$1.807 \pm 0.046 \pm 0.065$	$0.816 \pm 0.036 \pm 0.030$

0.007 ± 0.016 , from which we obtain the total branching fraction $\mathcal{B}(D_s^+ \rightarrow \phi e^+ \nu_e) = (2.61 \pm 0.03 \pm 0.08 \pm 0.15) \times 10^{-2}$. By comparing this quantity with the predicted decay rate, using the fitted parameters for the form factor pole ansatz we extract $A_1(0) = 0.607 \pm 0.011 \pm 0.019 \pm 0.018$. Here the third uncertainty refers to the combined value from external inputs, namely the branching fractions of the D_s^+ into $K^+ K^- \pi^+$ and of the ϕ into $K^+ K^-$, the D_s^+ lifetime $[(500 \pm 7) \times 10^{-15}\text{s}]$ and $V_{cs} = 0.9729 \pm 0.0003$. Predictions for this decay channel of lattice QCD calculations, in the quenched approximation [20], give: $r_V = 1.35_{-0.06}^{+0.08}$, $r_2 = 0.98 \pm 0.09$, $m_A = 2.42_{-0.16}^{+0.22}$ GeV/ c^2 and $A_1(0) = 0.63 \pm 0.02$. They agree with our determination of $A_1(0)$, r_2 and m_A , but are lower than the measured value of r_V . The measured form factor's ratio r_2 is in agreement with the value obtained for the same parameterization for the vector decay $D \rightarrow \bar{K}^* e^+ \nu_e$, whereas r_V is two standard deviations higher [8]. The branching fraction presented here agrees well with the value $(2.68 \pm 0.13)\%$, consistent with the assumption of equal semileptonic decay widths for the different charm mesons.

We are grateful for the excellent luminosity and machine conditions provided by our PEP-II colleagues, and for the substantial dedicated effort from the computing organizations that support BABAR. The collaborating institutions wish to thank SLAC for its support and kind hospitality. This work is supported by DOE and NSF (USA), NSERC (Canada), CEA and CNRS-IN2P3 (France), BMBF and DFG (Germany), INFN (Italy), FOM (The Netherlands), NFR (Norway), MES (Russia), MEC (Spain), and STFC (United Kingdom). Individuals have received support from the Marie Curie EIF (European Union) and the A. P. Sloan Foundation.

* Deceased

† Now at Temple University, Philadelphia, Pennsylvania 19122, USA

‡ Now at Tel Aviv University, Tel Aviv, 69978, Israel

§ Also with Università di Perugia, Dipartimento di Fisica, Perugia, Italy

¶ Also with Università di Roma La Sapienza, I-00185

Roma, Italy

** Now at University of South Alabama, Mobile, Alabama 36688, USA

†† Also with Università di Sassari, Sassari, Italy

- [1] B. Aubert *et al.*, *BABAR* Collaboration, Phys. Rev. **D76**, 052005 (2007).
- [2] Charge conjugate states are implied throughout this Letter.
- [3] K. Kodama *et al.*, E653 Collaboration, Phys. Lett. **B309**, 483 (1993).
- [4] P. L. Frabetti *et al.*, E687 Collaboration, Phys. Lett. **B328**, 187 (1994).
- [5] E.M. Aitala *et al.*, E791 Collaboration, Phys. Lett. **B450**, 294 (1999).
- [6] J.M. Link *et al.*, FOCUS Collaboration, Phys. Lett. **B586**, 183 (2004).
- [7] P. Avery *et al.*, CLEO Collaboration, Phys. Lett. **B337**, 405 (1994).
- [8] W.-M. Yao *et al.*, Particle Data Group, J. Phys. G **33**, 1 (2006).
- [9] Using a singlet-octet mixing angle of 39° , the branching fraction $\mathcal{B}(D^+ \rightarrow \phi e^+ \nu_e) \sim 2 \times 10^{-6}$ and we expect less than 10 events from this source in our data sample.
- [10] N. Cabibbo and A. Maksymowicz, Phys. Rev. **137**, B438 (1965).
- [11] C. L. Y. Lee, M. Lu and M. B. Wise, Phys. Rev. **D46**, 5040 (1992).
- [12] It is normalized such that: $\int_{m_\phi - \delta}^{m_\phi + \delta} (p^*/m) |\mathcal{A}_\phi(m)|^2 dm^2 \simeq 2 \arctan(2\delta/\Gamma_\phi^0)$ where δ is a small mass interval and Γ_ϕ^0 is the total width of the ϕ . The breakup momentum of the ϕ is denoted as p^* .
- [13] J. D. Richman and P. R. Burchat, Rev. Mod. Phys. **67**, 893 (1995).
- [14] M. Ablikim *et al.*, BES Collaboration, Phys. Lett. **B607**, 243 (2005).
- [15] B. Aubert *et al.*, *BABAR* Collaboration, Nucl. Instr. Methods Phys. Res., Sect. A **479**, 1 (2002).
- [16] S. Agostinelli *et al.*, Nucl. Instrum. Methods **A506**, (2003) 250.
- [17] T. Sjöstrand, Comp. Phys. Commun. **82**, 74 (1994).
- [18] E. Barberio and Z. Was, Comput. Phys. Commun. **79**, 291 (1994).
- [19] J. P. Alexander *et al.*, CLEO Collaboration, Phys. Rev. Lett. **100** 091801 (2008).
- [20] J. Gill, UKQCD Collaboration, Nucl. Phys. Proc. Suppl. **106**, 391 (2002).